Published in final edited form as:
J Mol Biol. 2010 July 9; 400(2): 204–217. doi:10.1016/j.jmb.2010.05.003.

Control of Catalytic Cycle by A Pair of Analogous tRNA Modification Enzymes

Thomas Christian[1], **Georges Lahoud**[1], **Cuiping Liu**[1], and **Ya-Ming Hou**[1,2]

[1]Thomas Jefferson University, Department of Biochemistry and Molecular Biology, 233 South 10th Street, BLSB 220, Philadelphia, PA 19107

Abstract

Enzymes that use distinct active site structures to perform identical reactions are known as analogous enzymes. The isolation of analogous enzymes suggests the existence of multiple enzyme structural pathways that can catalyze the same chemical reaction. A fundamental question concerning analogous enzymes is whether their distinct active-site structures would confer the same or different kinetic constraints to the chemical reaction, particularly with respect to the control of enzyme turnover. Here we address this question with the analogous enzymes of bacterial TrmD and its eukaryotic and archaeal counterpart Trm5. While both TrmD and Trm5 catalyze methyl transfer to synthesize the m1G37 base at the 3' position adjacent to the tRNA anticodon, using *S*-adenosyl methionine (AdoMet) as the methyl donor, TrmD features a trefoil-knot active-site structure whereas Trm5 features the Rossmann fold. Pre-steady-state analysis revealed that product synthesis by TrmD proceeds linearly with time, whereas that by Trm5 exhibits a rapid burst followed by a slower and linear increase with time. The burst kinetics of Trm5 suggests that product release is the rate-limiting step of the catalytic cycle, consistent with the observation of higher enzyme affinities to the products of tRNA and AdoMet. In contrast, the lack of burst kinetics of TrmD suggests that its turnover is controlled by a step required for product synthesis. Although TrmD exists as a homodimer, it showed "half-of-the-sites" reactivity for tRNA binding and product synthesis. The kinetic differences between TrmD and Trm5 are parallel to those between the two classes of aminoacyl-tRNA synthetases, which use distinct active-site structures to catalyze tRNA aminoacylation. This parallel suggests that the findings have a fundamental importance for enzymes that catalyze both methyl and aminoacyl transfer to tRNA in the decoding process.

Keywords

Trm5; TrmD; burst kinetics; tRNA(m1G37); half-of-the-site reactivity

Introduction

Enzymes use their active site structures to guide chemical conversion of substrates to products through several transition states. The unique local environments of each active site enforce specific orientations and conformations of the bound substrates to promote the chemical conversion, while also stabilizing the leaving groups in the formation of products. Enzymes

[2]Corresponding author: ya-ming.hou@jefferson.edu; phone: 215-503-4480;, fax: 215-503-5393.

that perform the same reaction usually share a highly conserved active site with sequence and structural features derived from the same evolutionary origin. However, exceptions to the rule exist, in which different active-site structures are recruited by enzymes of unrelated origins to catalyze the same chemical reaction [1]. When analogous enzymes of distinct structures are employed for the same reaction, a fundamental question is whether the difference in structures would influence the control of reaction kinetics. Of interest is the determination of the slowest step in a catalytic cycle that regulates the timing of turnover, which is associated with the highest activation energy barrier in the reaction coordinate.

The TrmD and Trm5 enzymes form an exemplary pair of analogous enzymes for the same reaction [2;3]. These enzymes catalyze methyl transfer from the methyl donor AdoMet to the N1 position of G37 to synthesize the modified m1G37 base 3' adjacent to the tRNA anticodon. TrmD is encoded by bacterial species and is characterized by an unusual AdoMet-binding fold that contains a rare protein subdomain known as the trefoil knot [4;5;6]. In contrast, Trm5 is encoded by eukaryotic and archaeal species and is characterized by the widely popular protein fold known as the Rossmann fold for binding the methyl donor [3;7;8;9]. The Rossmann fold and the trefoil knot structure share no common structural or sequence motifs and represent unrelated protein families[3;5;7]. In addition, TrmD exists as a homodimer with the two active sites assembled at the dimer interface [4;5], in which both monomers make substantial and interdigitating contributions to AdoMet binding. In contrast, Trm5 exists as a monomer and is active within a monomeric structure 3;10. With respect to tRNA recognition, these two enzymes also adopt different strategies: while Trm5 requires the integrity of the tRNA L shape, TrmD requires only a simple stem-loop structure mimicking the bottom half of the L shape [11]. Although there are other analogous pairs of tRNA modification enzymes, such as the pair consisting of the bacterial TrmJ (with a trefoil knot structure) and the eukaryotic Trm7 (with the Rossmann fold) for synthesis of 2'-*O*-methylation at position 32 of the anticodon loop [12], the TrmD-Trm5 pair is by far the best characterized.

The m1G37 modified base synthesized by TrmD and Trm5 is conserved in all three domains of life and is present in both the cytoplasm and mitochondria as one of the few tRNA modifications that are essential for growth [2;13;14;15;16]. The m1G37 modification plays multiple and important roles in translation: it enhances aminoacylation by archaeal cysteinyl- and phosphoseryl-specific aminoacyl-tRNA synthetases (aaRSs) [17;18], it prevents mis-charging of yeast $tRNA^{Asp}$ by ArgRS [19], and it accelerates entry of aminoacyl-tRNAs to the ribosome [20], while blocking frame-shifts of tRNA-ribosome complexes during translation [15;21]. The isolation of TrmD and Trm5 for the synthesis of m1G37 is significant, indicating the existence of separate structural pathways that arose early in evolution for the making of an essential modified base for tRNA maturation. Here, we use TrmD and Trm5 as examples of a pair of analogous enzymes to address how each controls the kinetics of the m1G37 synthesis reaction. We show that TrmD and Trm5 differ in the rate-limiting step of their catalytic cycle, and that their kinetic differences can be correlated with structural differences. Importantly, the structure-kinetic separation of TrmD from Trm5 is reminiscent of the previously observed separation between the two classes of aaRSs that catalyze aminoacyl transfer to tRNA [22]. Thus, the results of this study will have impact on enzymes that catalyze both aminoacyl transfer and methyl transfer to tRNA during the process of decoding genetic information.

Results

Separation of TrmD from Trm5 by pre-steady-state kinetics

We used *E. coli* TrmD and the archaeal *Methanococcus jannaschii* Trm5 as a representative pair for the synthesis of m1G37. Both enzymes are well characterized by x-ray crystal structures to have distinct AdoMet-binding folds [5;8;9]. In addition, the crystal structure of *M. jannaschii* Trm5 in complex with tRNA and AdoMet has recently been solved [9], which shows

base flipping of G37 from the anticodon loop into the active-site pocket. This base flipping is a common feature of all nucleic acid modification enzymes for which crystal structures are available. In steady-state kinetics, *E. coli* TrmD and *M. jannaschii* Trm5 have similar values of K_m with respect to both the tRNA and AdoMet substrates [3]. However, the lack of differentiation in steady state does not mean that these two enzymes share a similar kinetic mechanism, because steady-state analysis does not resolve individual steps in a catalytic cycle. Indeed, a separate single-turnover analysis of *M. jannaschii* Trm5 has shown that the enzyme exhibits a faster rate of methyl transfer than the steady-state rate [7], indicating that the steady-state rate does not report on methyl transfer for this enzyme. To better explore the kinetic mechanism of TrmD and Trm5 and to gain insight into the meaning of the steady-state rate, we examined pre-steady-state kinetics for these two enzymes. Because the preference for tRNA sequences for each enzyme differs, we chose the unmodified transcript of *E. coli* $tRNA^{Leu}$ as the substrate for TrmD and that of *M. jannaschii* $tRNA^{Cys}$ for Trm5, both of which are quantitatively modified by high concentrations of enzymes, indicating that they both have a well-folded structure [3;23].

The pre-steady-state analysis was performed with saturating AdoMet relative to the K_m of AdoMet for each enzyme. The tRNA substrate was maintained in a 10-fold molar excess of enzyme to permit one turnover of the reaction on the enzyme and subsequent steady-state synthesis. The amount of the m1G37-tRNA product synthesized was measured and calculated as the fraction (%) per active site of the enzyme. This analysis showed that while the synthesis of m1G37-tRNA by TrmD occurred in a time-dependent linear fashion, the synthesis by Trm5 occurred in a rapid burst phase followed by a slower and linear phase (Fig.1), demonstrating that the two enzymes are kinetically distinct. Fitting the TrmD data to a linear equation revealed a slope of $0.090 \pm 0.001\ s^{-1}$, which is the value of k_{cat} in steady state. Fitting the Trm5 data to a burst equation revealed a rate constant of $0.12 \pm 0.03\ s^{-1}$ for the first turnover and a rate constant of $0.020 \pm 0.007\ s^{-1}$ for the steady-state k_{cat}. The first turnover rate is defined as k_{chem}, which is a measure of the chemical conversion in the methyl transfer reaction under conditions of rapid binding equilibria. These k_{chem} and k_{cat} values of Trm5 are similar to the values determined separately from single-turnover and from steady-state analysis [7]. The observation of a k_{chem} greater than k_{cat} for Trm5 confirms that the steady-state k_{cat} does not represent the event of methyl transfer, but rather a physical step after the transfer. The active fraction of Trm5 was estimated at 20% based on the amplitude of the burst (Fig. 1); this corresponds closely to the previously reported plateau values for methyl transfer to the unmodified tRNA transcript [3]. The low levels of active fraction may be due to heterologous expression of *M. jannaschii* Trm5 in *E. coli*.

Tight binding of Trm5 to products

The burst kinetics of Trm5 suggests that the release of reaction products is slow such that it limits the rate of enzyme turnover. This was evaluated by determining the enzyme affinity for each substrate relative to the product. A higher affinity to the product than to the substrate would support the notion of slow product release. The equilibrium constant K_d of Trm5 for the tRNA substrate was determined from single turnover kinetics with increasing concentrations of the enzyme. All time courses of methyl transfer showed single exponential kinetics (Fig. 2A), confirming the rapid binding equilibria between the enzyme, tRNA and AdoMet. Fitting the data of rate as a function of Trm5 concentration to a hyperbolic equation yielded the maximum rate of $0.12 \pm 0.02\ s^{-1}$, consistent with the k_{chem} measured from pre-steady-state analysis, and an apparent K_d for the tRNA substrate of $0.7 \pm 0.1\ \mu M$ (Fig.2B), similar to the K_d reported previously [7].

The K_d of Trm5 for the m1G37-tRNA product was determined by treating the product as an inhibitor of the methyl transfer reaction. The m1G37-tRNA product was synthesized from the

methyl transfer reaction and was purified away from the unreacted substrate by a previously developed method [24]. It was used to form a series of Trm5-product complexes that was assayed for the m1G37 synthesis activity in pre-steady-state kinetics. While increasing concentration of the product had little effect on the rate of the burst or steady-state phase, it progressively decreased the amplitude of the burst phase (Fig.2C), indicating that the dissociation of the product from Trm5 was slow such that it limited the availability of the enzyme for the methyl transfer reaction. A fit of the data to a quadratic equation yielded a K_d of 0.2 ± 0.1 μM of the enzyme-product complex (Fig.2D), lower than the K_d (0.7 ± 0.1 μM) of the enzyme-substrate complex by 3–4-fold. This result demonstrates the tight binding affinity of Trm5 for the m1G37-tRNA product.

The methyl transfer reaction converts AdoMet to *S*-adenosyl homocysteine (AdoHcy). The K_d constants of the enzyme for AdoMet and AdoHcy were determined to address the affinity for each. The K_d for AdoMet was determined by formation of a series of Trm5-AdoMet complexes that was used to monitor the m1G37 synthesis reaction in pre-steady state. As the AdoMet concentration increased, the amplitude of the burst phase also increased (Fig.3A), indicating the enzyme dependence on AdoMet binding for the methyl transfer activity. Fitting the amplitude data as a function of AdoMet concentration to a hyperbolic equation revealed a K_d of 0.44 ± 0.09 μM for AdoMet (Fig.3B). Determination of K_d for AdoHcy was determined similarly to that for the m1G37-tRNA product. A series of Trm5-AdoHcy complexes was preformed and used to inhibit the m1G37 synthesis reaction. While the increase in the concentration of AdoHcy had little effect on the burst or steady-state rate, it progressively decreased the amplitude of the burst phase (Fig.3C). Fitting the amplitude data *vs*. the concentration of AdoHcy to a hyperbolic equation revealed a K_d of 20 ± 5 nM (Fig.3D), which is nearly 20-fold lower than the K_d of 0.44 ± 0.09 μM for AdoMet (Fig.3B), demonstrating the preferential tight binding of Trm5 to AdoHyc than to AdoMet. In fact, analysis of the K_d values of the two products reveals that Trm5 affinity for AdoHcy is higher than that for the m1G37-tRNA product (K_d = 0.2 ± 0.1 μM) by 20-fold, indicating a specific role of AdoHcy in product release.

Kinetics of TrmD and stoichiometry of product formation

The lack of burst kinetics of TrmD suggests that the steady-state turnover rate k_{cat} is not limited by product release. To better understand the meaning of k_{cat}, the rate of methyl transfer was measured from single turnover kinetics. All time courses of m1G37 synthesis showed single exponential kinetics (Fig.4A), indicating that the formation of TrmD-tRNA-AdoMet complexes was in rapid equilibrium binding and that the kinetics of the reaction was not limited by binding but by the rate of methyl transfer. Fitting the data of rate as a function of the TrmD dimer concentration to a hyperbolic equation revealed the maximum rate constant k_{chem} of 0.090 ± 0.003 s^{-1} (Fig.4B), virtually identical to the k_{cat} determined in pre-steady state (Fig. 1). Thus, the steady-state k_{cat} of TrmD is defined by the rate of methyl transfer. An active-site titration of TrmD revealed that the dimer was 72 ± 5 % active (Supplementary information, Fig.S1), which was used to correct the enzyme concentration in single turnover kinetics. From the titration of rate *vs*. concentration, a K_d of 0.44 ± 0.09 μM for the TrmD-tRNA complex was identified (Fig.4B), well within the physiological concentrations of tRNA. All of the kinetic parameters for TrmD and Trm5 obtained here are summarized in Table 1.

Because TrmD functions as a dimer, the stoichiometry of m1G37 synthesis is of interest. This was determined by measuring the amount of m1G37 synthesis per TrmD dimer at the time point that allowed one turnover (11 sec). A saturating concentration of tRNA relative to the K_d (tRNA) was used to react with a series of high concentrations of TrmD dimer to establish rapid equilibrium binding. Analysis of the synthesis of m1G37-tRNA as a function of TrmD dimer revealed two phases of linear relationships (Fig.5). The first phase was observed under

conditions where tRNA was in excess of the TrmD dimer and the slope of this phase was 0.93. Thus, despite the molar excess of tRNA relative to the enzyme dimer, each dimer synthesized approximately only one m1G37 on tRNA in one turnover. This unexpected result suggests that TrmD exhibits "half-of-the-sites" reactivity in which only one of the two active sites is functional at a given time. If both active sites were to function equivalently at the same time, then each dimer should have synthesized two molecules of the product. The second linear phase in the titration was observed under conditions where enzyme was in excess of tRNA. The slope of this linear phase (0.34) was less than one, which was expected because each dimer can react with less than one tRNA in conditions of limiting concentrations of tRNA.

Fluorescence analysis of substrate binding to TrmD

To determine the molecular basis for the half-of-the-sites reactivity of TrmD, the binding stoichiometries for AdoMet and tRNA were determined by equilibrium titrations of intrinsic tryptophan fluorescence. For measurement of AdoMet binding, the fluorescence was excited at 295 nm and the emission was monitored at 310–400 nm. Because AdoMet binding showed little absorption at either wavelength, the peak of each emission (at 330 nm) was recorded directly and corrected for dilution. Titration of TrmD with increasing concentrations of AdoMet showed that the binding progressively quenched the intrinsic fluorescence and that fitting the data to a quadratic binding equation yielded a K_d of 1.1 ± 0.2 μM for the methyl donor (Fig.6A). The stoichiometry of AdoMet binding was then determined by using a high concentration of TrmD relative to the K_d (AdoMet) to drive the binding interaction. Analysis of the fluorescence data *vs*. the molar ratio of AdoMet relative to the dimer revealed a biphasic quenching curve (Fig.6B), in which the first phase of quenching was steep and linear with respect to the molar ratio up to the value of 2, while the second phase was flat and independent of the increase in molar ratio. The value of 2 in the first phase indicates that, in the absence of tRNA, each TrmD dimer is capable of binding two molecules of AdoMet, which is consistent with the finding in crystal structures of TrmD and suggests that the dimer is symmetrical with respect to AdoMet binding. The flat second phase indicates that, once the stoichiometry of 2 is reached, there is no further binding of AdoMet to the enzyme.

For measurement of tRNA binding, quenching of intrinsic tryptophan fluorescence was also observed and the data was similarly recorded as in the case of AdoMet, except that the magnitude of each emission peak (at 330 nm) was corrected for dilution and for inner filter effect, due to absorption of tRNA at the excitation and emission wavelengths. Fitting the fluorescence quenching data to a quadratic equation yielded a K_d of 0.30 ± 0.03 μM for tRNA (Fig.6C), similar to the value obtained by kinetics (Fig.4B). The stoichiometry of tRNA binding was then determined by using a high concentration of TrmD relative to the K_d (tRNA) to drive the binding interaction. Analysis of fluorescence data as a function of the molar ratio of tRNA to the dimer also revealed a biphasic quenching curve (Fig.6D). The initial quenching was steep and linear with respect to the molar ratio up to the value of 1, which was followed by a much flatter second phase. These data indicate that each TrmD dimer can specifically bind only one tRNA, and that the further fluorescence quenching at higher tRNA concentrations is probably due to non-specific binding interactions. The stoichiometry of one tRNA binding per dimer is consistent with the stoichiometry of methyl transfer. Thus, while the two subunits of TrmD can both simultaneously bind AdoMet, only one can bind tRNA at a time to perform the methyl transfer reaction.

The fluorescene titration method was also used to determine TrmD affinities for the products AdoHcy and m1G37-tRNA. Binding of AdoHcy to TrmD dimer under a condition similar to that of AdoMet binding revealed quenching of the intrinsic fluorescence (Fig.6E). Fitting the fluorescence quenching data *vs*. AdoHcy concentration to a quadratic equation revealed a K_d of 0.33 ± 0.04 μM, indicating a 3–4-fold higher affinity relative to the K_d of 1.1 ± 0.2 μM for

AdoMet. However, this 3–4-fold higher affinity is smaller in magnitude than the 20-fold higher affinity in the case of Trm5 with respect to binding AdoHcy *vs*. AdoMet. Interestingly, for the m1G37-tRNA product, while fluorescence quenching was also observed upon binding of this product, a fit of the fluorescence quenching data (after correction of inner filter effect) *vs*. the concentration of m1G37-tRNA to a quadratic equation revealed a K_d of 40 ± 2 nM, indicating a ~10-fold higher affinity relative to the K_d of 0.30 ± 0.03 μM for tRNA. The fluorescence binding K_d values for both substrates and products of TrmD are summarized in Table 1.

Discussion

Distinct kinetic control of catalytic cycle by TrmD and Trm5

The goal of this study was to address the question of whether enzymes with distinct structural folds would impose the same or different control of their catalytic cycle for the same chemical reaction. Using TrmD and Trm5 as an exemplary pair, we examined their control of the catalytic cycle by pre-steady-state kinetics and applied the rate constant k_{chem} to encompass all of the steps required for product synthesis and the constant k_{cat} for those involved in product release. For the m1G37 synthesis reaction, k_{chem} includes the terms for substrate binding, active site rearrangement, base flipping of G37, deprotonation of N1 of G37, and methyl transfer to N1 from AdoMet, whereas k_{cat} also includes the terms for breakdown of the ternary complex with m1G37-tRNA and AdoHcy and the release of products from the enzyme. Here we show that Trm5 exhibits burst kinetics and that it has preferential binding affinities to the reaction products relative to the respective substrates, indicates that this enzyme uses the rate-limiting product release step to control its catalytic cycle. In contrast, we show that TrmD lacks the burst kinetics and that it exhibits identical rates for the synthesis and release of products, indicating that this enzyme uses the rate-limiting product synthesis to control its catalytic cycle. Thus, the two enzymes exert different kinetic controls of their catalytic cycle.

The distinction between TrmD and Trm5 is reminiscent of the distinction between the two classes of aaRSs in both structure and kinetics. The family of aaRSs includes the 20 canonical enzymes, each of which uses the energy of ATP hydrolysis to activate an amino acid substrate and to transfer the activated aminoacyl-adenylate to the 3' end of cognate tRNAs to synthesize aminoacyl-tRNAs as substrates for protein synthesis [25]. Class I aaRSs bind ATP in the Rossmann fold, whereas class II aaRSs bind ATP in a non-Rossmann fold created by the interface of oligomeric subunits (typically homodimers). Such class-specific structural features of aaRSs are recognizable in ways that separate TrmD from Trm5 and are directly relevant to the spatial binding of ATP or AdoMet, which share in common an adenosine moiety that is likely to provide fundamental constraints in the rate of chemical conversion and the rate of catalytic turnover. Indeed, structural analysis of these enzymes has consistently shown that enzymes of the same active-site structure bind AdoMet (Fig.7A,B) or ATP (Fig.7C,D) in a similar conformation. Specifically, the Rossmann fold in methyl transferases binds AdoMet in an extended conformation with a degree of 160–180° for the C4'-C5'-Sδ-Cγ dihedral angle (Fig.7A) [8;9], similar to the extended conformation of ATP in the Rossmann fold of aaRSs (Fig. 7C) [26]. In contrast, the non-Rossmann fold in methyl transferases binds AdoMet in a bent conformation with an ~80° degree of the dihedral angle mentioned above (Fig.7B), similar to the bent conformation of ATP in the non-Rossmann fold of aaRSs (Fig.7D) [27]. In parallel, kinetic analysis has consistently shown that enzymes of the Rossmann-fold active site exhibit burst kinetics, such as class I aaRSs22, while enzymes of the non-Rossmann fold active site assembled at the interface of oligomeric subunits lack burst kinetics, such as class II aaRSs22;28;29. Together, these results form a large database to unite enzymes of diverse functions (methyl transfer and aminoacyl transfer) to derive a model for correlating structure with kinetics. This model proposes that the extended conformation of AdoMet or ATP in the Rossmann fold favorably positions the relevant reactive groups for facile chemical conversion

involving bond breaking and bond formation to occur. This leaves open a suitable approach for the deprotonated nucleophile of the target base to the methyl group of AdoMet in the methyl transfer reaction or the deprotonated α-phosphate to the carbonyl group of ATP in the aminoacylation reaction. In contrast, the bent conformation of AdoMet or ATP in the non-Rossmann fold does not leave such access for the incoming nucleophile. The facile structural environment to promote chemistry in the Rossmann fold has been previously noted by structural and kinetic analysis for class I aaRSs [22], whereas the requirement of structural re-organization prior to chemistry in the non-Rossmann fold has also been noted for class II aaRSs [28;29]. Broad support for the model is the observation that, while Trm5 is the first Rossmann-fold RNA methyl transferase to be characterized kinetically, several DNA methyl transferases with the same fold also show burst kinetics and slow product release [30;31;32;33]. However, exceptions to the rule might exist, but detailed structural and kinetic analysis must be performed to address how the exceptions occur. For example, SepRS is a tetramer that uses a non-Rossmann fold active site to catalyze aminoacylation of $tRNA^{Cys}$ with phosphoserine to synthesize sep-$tRNA^{Cys}$ as an intermediate in the pathway for cys-$tRNA^{Cys}$ biosynthesis [34]. SepRS exhibits burst kinetics [18], indicating an exception to the no-burst rule of non-Rossmann enzymes, but the basis for the exception is not known, because there is no structural data showing the geometry of the ATP bound in the active site [35;36]. Thus, it is important to recognize that, while further data are needed to address possible exceptions, the proposed model serves as a useful foundation to relate how each structure confers the specific kinetic property.

Product release from Trm5

Burst kinetics has been used as a tool to measure the affinities of Trm5 to AdoMet and tRNA, and to the respective products of these substrates. The advantage of this method is that the binding of substrates to Trm5 was fast and under the diffusion control so that the reaction kinetics could be used to monitor the extent of binding. Another advantage is that affinities were measured in the catalytically competent state of Trm5 during the reaction of methyl transfer. The observation that Trm5 binds with a 3–4 fold higher affinity to m1G37-tRNA relative to tRNA, and with a ~20-fold higher affinity to AdoHcy relative to AdoMet, is consistent with the existence of a highly stable ternary product complex of the enzyme with m1G37-tRNA and AdoHcy, which is slow to release the products. Of significance is the particularly tight binding of Trm5 to AdoHcy (K_d = 20 nM), indicating that the release of this product is the dominant factor in the overall catalytic turnover. A similar case is found in the related DNA methyl transferase M.HhaI (responsible for synthesis of m5C in DNA), where the release of AdoHcy is the slowest in the catalytic cycle and it occurs before the release of the methylated DNA product [37;38], indicating that as soon as AdoHcy is released, the release of the nucleic acid product quickly follows. This order of release is likely to apply to Trm5 as well.

A possible rationale for the dominance of AdoHcy in the Trm5 turnover is discernable by biochemical and structural analysis of the enzyme. The recent ternary complex of Trm5 with AdoMet and tRNA reveals that the methyl donor is tightly bound in the active site (Fig.7A) 9, where the adenine ring and the ribose 2'- and 3'-OH groups of the adenosine moiety are each anchored by conserved motifs of the Rossmann fold (such as D223, I224, D251, and F203), while the carboxyl and amino groups of the methionine moiety are each stabilized by interactions with N265 and P267 of the catalytic NLP loop (analogous to the NPPY loop of other Rossmann-fold enzymes 39). It is in this intimate interaction network that AdoMet is positioned for methyl transfer to generate AdoHcy. Superposition of the ternary structure of Trm5 with a binary structure 8 bound to the analog sinefungin reveals a major difference in the ordering of the K137-R147 loop, which moves in closer to the bound AdoMet in the tertiary complex (by ~2 Å) and helps to stabilize the flipped-in G37 base. The structural change of the

loop is important in the ternary complex to enforce tighter interactions with the methyl donor, and is consistent with the observed affinity improvement of AdoMet to Trm5 in the presence of tRNA (K_d = 0.44 μM, Table 1) than in the absence of tRNA (K_d = 3.1 μM) as determined previously [7]. The conformation change of the K137-R147 loop in the active-site by the presence of tRNA is coupled with distal induced-fit movements, including the enzyme contacts with the tRNA tertiary core and those with the D and anticodon stem-loop backbone groups 9, suggesting that the binding of the entire tRNA is optimized to position the catalytic NLP loop to "lock" on the methyl donor. Importantly, in the related Rossmann-fold structures of M.HhaI methyl transferase, the structurally stabilized enzyme lock on AdoMet is essentially unchanged as AdoMet is converted to AdoHcy 40;41;42, even though the stereochemical position of the lock can change in the course of methyl transfer. This provides insight into how the enzyme structure is designed to lock on virtually all parts of the AdoMet molecule (both the adenosine and methionine moieties) such that the release of AdoHcy after methyl transfer would be the most critical step in the breakdown of the product complex.

Product synthesis by TrmD

The determination that TrmD exhibits identical rate constants k_{chem} and k_{cat} (Table 1) indicates that the methyl transfer event on the enzyme is slow relative to product release such that k_{chem} dominates k_{cat}. A key feature of the methyl transfer by TrmD is the half-of-the-sites reactivity, where although both active sites of the homodimeric enzyme are capable of binding AdoMet, only one binds tRNA and only one catalyzes methyl transfer (Fig.6). The origin of the half-of-the-sites reactivity is not known at present, due to the lack of tRNA-bound crystal structure. Note that while the two active sites of TrmD are identical upon AdoMet or AdoHcy binding in binary crystal structures of TrmD4;5, this symmetry may result from crystal packing forces and does not exclude the possibility of a pre-existing asymmetry prior to tRNA binding. Alternatively, the half-of-the-sites reactivity may arise during tRNA binding to a preexisting symmetric dimer to the highly interdigitating and expansive interface of the two monomers (accounting for 26% of the total surface per monomer), which may form the binding surface for the G37 base and may be constructed in such a way to allow only one tRNA to bind to one subunit or alternatively bind across the dimer interface, leading to the stoichiometry of one tRNA bound per dimer. Half-of-the-sites activity has been previously shown for dimeric and tetrameric aaRSs of both the Rossmann-fold and the non-Rossmann-fold type [17;28;29;43;44;45]. The discovery of half-of-the-sites reactivity for TrmD suggests that this phenomenon may be general to multimeric enzymes that operate on tRNA.

The structural basis for the tRNA-induced asymmetry of TrmD cannot be resolved by the present data and further experiments are necessary. One possibility of the asymmetry is an oscillating model, in which the two active sites are both active and the one with the bound G37 of tRNA catalyzes methyl transfer and the synthesis of m1G37-tRNA on the subunit activates the second subunit to bind to a new G37 in a different tRNA, which then triggers the release of the m1G37-tRNA product from the first subunit. The K_d values determined from fluorescence titration are consistent with some aspects of this oscillating model, showing that a TrmD dimer binds the m1G37-tRNA product with a ~10-fold higher affinity (K_d = 40 ± 2 nM) relative to the affinity for the tRNA substrate (K_d = 0.3 ± 0.03 μM) (Fig.6C, F). Because the catalytic cycle of TrmD is not limited by product release, the tight binding of the m1G37-tRNA product on one subunit can serve to activate the second subunit to bind to a new tRNA substrate. Note that because the fluorescence analysis presented here was performed with just the enzyme-product or enzyme-substrate complexes, it cannot be used to determine the enzyme-product affinity upon binding of a second molecule of substrate. New fluorescence tools are being developed to address the dynamics of the two subunits in the oscillating model. Other possibilities of the asymmetry of TrmD also exist. For example, a variation of the oscillating model is that the one subunit with the bound G37 of tRNA does not catalyze methyl

transfer but moves the nucleic acid substrate to the second active site to perform methyl transfer. Alternatively, the two active sites can be unequal upon tRNA binding and only one of the two is active for methyl transfer.

Implications for biology

This study demonstrates that the analogous enzymes TrmD and Trm5 control their catalytic cycle by distinct kinetic steps that are directly related to their unique active-site structures. While TrmD controls its catalytic cycle by the rate of methyl transfer, Trm5 controls the cycle by coordinating the release of AdoHcy. The specific control may serve a useful biological function for each enzyme. For example, the half-of-the-sites reactivity of TrmD can be considered an extreme case of negative cooperativity, as has been suggested for dimeric aaRSs that exhibit this property 46. The half-of-the-sites reactivity of TrmD occurs at the tRNA binding step, suggesting that the negative cooperativity between the two subunits with respect to tRNA binding would confer the enzyme a high sensitivity to intracellular changes of tRNA concentrations, such as those occurring in stress conditions that can drastically curtail biosynthesis of tRNA [47]. Because TrmD is proposed to act early in the pathway of tRNA maturation (due to its ability to synthesize m1G37 without complete folding of tRNA) [9], this innate sensitivity to reduced tRNA levels in stress conditions can help to establish an early decision point to arrest the m1G37 synthesis and to terminate the maturation pathway so as to eliminate the cellular expenditure for further modification reactions. Conversely, the kinetic control of Trm5 in product release is relevant to the utility of the m1G37-tRNA product as the obligate precursor for synthesis of the complex wybutosine base in $tRNA^{Phe}$ at the 37 position [48]. The slow product release by Trm5 may be a strategy to protect the m1G37-tRNA product and to channel it to the downstream enzyme in the wybutosine biosynthesis pathway. Similar models for the channeling are the two-step reaction pathways that synthesize certain aminoacyl-tRNAs by the action of two enzymes [18;49], where the aaRS for the first reaction delays product release and facilitate product transfer to the second enzyme in order to promote rapid production of the end product. Importantly, the wybutosine modification in $tRNA^{Phe}$ is conserved in eukaryotes and archaea but is absent from bacteria, consistent with the biological distribution of Trm5 and supporting a role of Trm5 in the biosynthesis pathway of the modification.

Methods

Material preparation

E. coli TrmD with an N-terminal His tag and *M. jannaschii* Trm5 with a C-terminal His tag were expressed and purified as described [3; 23]. Transcripts of *E. coli* $tRNA^{Leu}$ and *M. jannaschii* $tRNA^{Cys}$ were prepared and purified as described [11]. [^{3}H-methyl]-AdoMet was purchased from Perkin Elmer (NET155H, 70.8 Ci/mmol).

Kinetic assays

The synthesis of m1G37-tRNA by *M. jannaschii* Trm5 was performed at 55 °C in a buffer containing 100 μM Tris-HCl, pH 8.0, 4 mM DTT, 0.1 mM EDTA, 6 mM $MgCl_2$, 100 mM KCl, and 0.024 mg/mL BSA. The synthesis by *E. coli* TrmD was performed at 37 °C in the same buffer except for the substitution of 100 mM KCl with 24 mM NH_4Cl. The tRNA substrate was heat-denatured at 85 °C for 3 min and annealed at 37 °C for 15 min before use. Pre-steady-state and single turnover experiments were monitored upon rapid mixing of 15 μL of enzyme in one syringe with 15 μL of a mixture of annealed tRNA and ^{3}H-AdoMet in the second syringe on the RQF-3 rapid quench instrument (KinTek Corp, Texas). The reaction was quenched with 54 μL of 5% trichloroacetic acid (TCA) and an aliquot of 20 μL was spotted on a Whatman filter pad, which was washed several times with 5% TCA, dried, and counted

in a scintillation counter. The ^{3}H-m1G37-tRNA precipitated on the filter pad was determined and quantified.

Burst kinetics

Pre-steady-state kinetics of m1G37-tRNA synthesis was monitored upon rapid mixing of enzyme (1 μM) in one syringe with an annealed tRNA (10 μM) and ^{3}H-AdoMet (50 μM) in the second syringe on the RQF-3 instrument. Data of Trm5 were fit to the burst equation: $y = y_o + A\times (1 - e^{-k1\times t}) + k_2 \times E_o \times t$, where y_o is the y intercept, A is the amplitude of the initial exponential phase, k_1 is the apparent rate constant of the initial exponential regression, k_2 is the apparent rate constant of the steady-state phase, and t is the time in seconds [22;50].

Single turnover kinetics

Single turnover kinetics was performed by rapid mixing of enzyme (2–25 μM) in one syringe with tRNA (0.25 μM) and AdoMet (25 μM) in the second syringe. Data were fit to the single exponential equation: $y = y_o + A \times (1-e^{-kapp\times t})$ where y_o is the y intercept, A is the scaling constant, k_{app} is the apparent rate constant, and t is the time in seconds to determine k_{app} [22; 50]. Control experiments confirmed that the mixing order of enzyme, tRNA, and AdoMet does not affect the rate of methyl transfer. The data of k_{app} *vs*. enzyme concentration for single turnover analysis of m1G37-tRNA synthesis were fit to the hyperbolic equation: $y = k_{chem} \times E_o /(E_o + K_d)$, where k_{chem} is the rate constant for the chemistry step, and E_o is the enzyme concentration [22;50].

Measurement of K_d for m1G37-tRNA

Measurement of the K_d for m1G37-tRNA was obtained by pre-steady-state analysis, in which a series of enzyme (1 μM)-product (0–1.5 μM) complexes (preformed at 37 °C, 30 min) in one syringe was rapidly mixed with tRNA (annealed at 37 °C, 15 min) and AdoMet (50 μM) in the second syringe to initiate the m1G37 synthesis reaction. Data of the burst amplitude as a function of the product tRNA was fit to a quadratic equation:

$$y=y_o - \Delta y \times \frac{(E_o+I+K_d) - \sqrt{(E_o+I+K_d)^2 - 4 \times E_o \times I}}{2 \times E_o}$$

where y_o is the initial amplitude without the inhibitor m1G37-tRNA, $\otimes y$ is the scaling constant for amplitude change, E_o is the initial enzyme concentration, I is the concentration of m1G37-tRNA[22; 50]

Measurement of K_d for AdoMet

Measurement of the K_d for AdoMet was obtained by pre-steady-state analysis, in which a series of enzyme (5 μM)-AdoMet (0.5–20 μM) complexes (at 37 °C, 30 min) in one syringe was rapidly mixed with tRNA (annealed at 37 °C, 15 min) in the second syringe to initiate the m1G37 synthesis reaction. Data of the burst amplitude as a function of AdoMet concentration was fit to the hyperbolic equation: $y = A \times S /(S + K_d)$; where A is maximum amplitude in burst kinetics, S is the AdoMet concentration [22;50].

Measurement of K_d for AdoHcy

Measurement of the K_d for AdoHcy was obtained by pre-steady-state analysis, in which a series of enzyme (5 μM)-AdoHcy (10–200 nM) complexes (at 37 °C, 30 min) in one syringe was rapidly mixed with tRNA (annealed at 37 °C, 15 min) and AdoMet (25 μM) in the second syringe to initiate the m1G37 synthesis reaction. Data of the burst amplitude as a function of AdoHcy was fit to the hyperbolic equation: $y = y_o - A \times I/(I + K_d)$; y_o is the initial burst amplitude

in the absence of AdoHcy; *A* is the scaling constant for amplitude change upon addition of AdoHcy; *I* is the concentration of AdoHcy [22;50].

Active site titration and stoichiometry of methyl transfer

Enzyme (100 nM) in one syringe was rapidly mixed with tRNA (10–300 nM) and AdoMet (30 μM, specific activity 1990 dpm/pmol) in the second syringe in a total volume of 20 μL to initiate methyl transfer. An aliquot of the reaction (15 μL) was quenched by acid after the time period that allowed for one cycle of methyl transfer (11 sec) and was analyzed by a scintillation counter to determine the amount of m1G37-tRNA synthesis. The data were fit to the following equation to derive the active fraction: $y=\frac{(E_o+S+K_d)-\sqrt{(E_o+S+K_d)^2-4\times E_o\times S}}{2}$, where *y* represents the methylated tRNA product after one turnover; *Eo* is the active enzyme concentration; *S* is the tRNA concentration; K_d is the dissociation constant for tRNA [22;50].

The stoichiometry of methyl transfer was determined by rapid mixing of active enzyme dimer (0, 0.36, 0.72, 1.08, 1.44, 1.8, 2.16, 3.6, 5.76, and 9.0 μM) in one syringe with tRNA (5 μM) and AdoMet (30 μM, 1900 dpm/pmol) in the second syringe on the RFQ-3 instrument in a time course up to 55 sec. The progress curve of the synthesis of m1G37-tRNA synthesis at 0, 1, 3, 6, 9, 10, 11, 12, 16, 20, 30, 40, and 55 sec was sampled and fit to the hyperbola for single turnover kinetics (see above). The amount of m1G37-tRNA synthesis at 11 sec was determined from the progress curve and plotted as a function of the dimer concentration.

Fluorescence titration experiments

The stoichiometry of TrmD binding to substrates and products was determined by monitoring the quenching of intrinsic tryptophan fluorescence. The fluorescence was excited at 295 nm and the emission was monitored from 304 nm to 400 nm at room temperature in a buffer containing 100 mM Tris-HCl, pH 8.0, 100 mM KCl, 0.1 mM EDTA, 6 mM $MgCl_2$, and 4 mM DTT. For K_d measurements, TrmD was at 0.2 μM and AdoMet and AdoHcy were both titrated in the range of 0.1–40 μM. while the $tRNA^{Leu}$ transcript was titrated in the range of 0.1–6 μM. For measurement of the K_d of m1G37-tRNA, the product tRNA was synthesized and purified by a previously developed method [24] and was titrated in the range of 0.011–0.6 μM against 0.05 μM TrmD. The data were fit to the quadratic equation using Kaleidagraph:

$F=F_o-\Delta F\times\frac{(E_o+S+K_d)-\sqrt{(E_o+S+K_d)^2-4\times E_o\times S}}{2\times E_o}$, where *F* is the measured fluorescence signal; F_o stands for the initial fluorescence before the addition of enzyme; ΔF represents the scale of fluorescence signal change; E_o is the initial enzyme concentration; S is the tRNA or AdoMet concentration [22;50]. For stoichiometry determination, AdoMet was titrated in the range of 0–103 μM for TrmD dimer (10 μM), and tRNA was titrated in the range 0–12.4 μM for TrmD dimer (2.9 μM). For analysis of the stoichiometry of AdoMet, the emission peak at 330 nm was recorded and corrected for dilution. For analysis of the stoichiometry of tRNA, the emission peak at 330 nm was corrected additionally for inner filter effect, according to the formula, $F_c = F_{obs} \times anti\log((A_{295} + A_{330})/2)$.

Supplementary Material

Refer to Web version on PubMed Central for supplementary material.

Acknowledgments

We thank Chris Francklyn, John Perona, and Paul Schimmel for discussion and Howard Gamper for comments on the manuscript. Supported by NIH grant GM081601 to YMH.

References

1. Galperin MY, Walker DR, Koonin EV. Analogous enzymes: independent inventions in enzyme evolution. Genome Res 1998;8:779–790. [PubMed: 9724324]
2. Bjork GR, Jacobsson K, Nilsson K, Johansson MJ, Bystrom AS, Persson OP. A primordial tRNA modification required for the evolution of life? Embo J 2001;20:231–239. [PubMed: 11226173]
3. Christian T, Evilia C, Williams S, Hou YM. Distinct origins of tRNA(m1G37) methyltransferase. J Mol Biol 2004;339:707–719. [PubMed: 15165845]
4. Ahn HJ, Kim HW, Yoon HJ, Lee BI, Suh SW, Yang JK. Crystal structure of tRNA(m1G37) methyltransferase: insights into tRNA recognition. Embo J 2003;22:2593–2603. [PubMed: 12773376]
5. Elkins PA, Watts JM, Zalacain M, van Thiel A, Vitazka PR, Redlak M, Andraos-Selim C, Rastinejad F, Holmes WM. Insights into catalysis by a knotted TrmD tRNA methyltransferase. J Mol Biol 2003;333:931–949. [PubMed: 14583191]
6. Anantharaman V, Koonin EV, Aravind L. SPOUT: a class of methyltransferases that includes spoU and trmD RNA methylase superfamilies, and novel superfamilies of predicted prokaryotic RNA methylases. J Mol Microbiol Biotechnol 2002;4:71–75. [PubMed: 11763972]
7. Christian T, Evilia C, Hou YM. Catalysis by the second class of tRNA(m1G37) methyl transferase requires a conserved proline. Biochemistry 2006;45:7463–7473. [PubMed: 16768442]
8. Goto-Ito S, Ito T, Ishii R, Muto Y, Bessho Y, Yokoyama S. Crystal structure of archaeal tRNA(m(1) G37)methyltransferase aTrm5. Proteins 2008;72:1274–1289. [PubMed: 18384044]
9. Goto-Ito S, Ito T, Kuratani M, Bessho Y, Yokoyama S. Tertiary structure checkpoint at anticodon loop modification in tRNA functional maturation. Nat Struct Mol Biol 2009;16:1109–1115. [PubMed: 19749755]
10. Brule H, Elliott M, Redlak M, Zehner ZE, Holmes WM. Isolation and characterization of the human tRNA-(N1G37) methyltransferase (TRM5) and comparison to the Escherichia coli TrmD protein. Biochemistry 2004;43:9243–9255. [PubMed: 15248782]
11. Christian T, Hou YM. Distinct determinants of tRNA recognition by the TrmD and Trm5 methyl transferases. J Mol Biol 2007;373:623–632. [PubMed: 17868690]
12. Purta E, van Vliet F, Tkaczuk KL, Dunin-Horkawicz S, Mori H, Droogmans L, Bujnicki JM. The yfhQ gene of Escherichia coli encodes a tRNA:Cm32/Um32 methyltransferase. BMC Mol Biol 2006;7:23. [PubMed: 16848900]
13. Lee C, Kramer G, Graham DE, Appling DR. Yeast mitochondrial initiator tRNA is methylated at guanosine 37 by the Trm5-encoded tRNA (guanine-N1-)-methyltransferase. J Biol Chem 2007;282:27744–27753. [PubMed: 17652090]
14. Baba T, Ara T, Hasegawa M, Takai Y, Okumura Y, Baba M, Datsenko KA, Tomita M, Wanner BL, Mori H. Construction of Escherichia coli K-12 in-frame, single-gene knockout mutants: the Keio collection. Mol Syst Biol 2006;2:0008. [PubMed: 16738554]
15. Bjork GR, Wikstrom PM, Bystrom AS. Prevention of translational frameshifting by the modified nucleoside 1-methylguanosine. Science 1989;244:986–989. [PubMed: 2471265]
16. O'Dwyer K, Watts JM, Biswas S, Ambrad J, Barber M, Brule H, Petit C, Holmes DJ, Zalacain M, Holmes WM. Characterization of Streptococcus pneumoniae TrmD, a tRNA methyltransferase essential for growth. J Bacteriol 2004;186:2346–2354. [PubMed: 15060037]
17. Hauenstein SI, Hou YM, Perona JJ. The homotetrameric phosphoseryl-tRNA synthetase from Methanosarcina mazei exhibits half-of-the-sites activity. J Biol Chem 2008;283:21997–22006. [PubMed: 18559342]
18. Zhang CM, Liu C, Slater S, Hou YM. Aminoacylation of tRNA with phosphoserine for synthesis of cysteinyl-tRNA(Cys). Nat Struct Mol Biol 2008;15:507–514. [PubMed: 18425141]
19. Putz J, Florentz C, Benseler F, Giege R. A single methyl group prevents the mischarging of a tRNA. Nat Struct Biol 1994;1:580–582. [PubMed: 7634096]
20. Li J, Esberg B, Curran JF, Bjork GR. Three modified nucleosides present in the anticodon stem and loop influence the in vivo aa-tRNA selection in a tRNA-dependent manner. J Mol Biol 1997;271:209–221. [PubMed: 9268653]

21. Urbonavicius J, Qian Q, Durand JM, Hagervall TG, Bjork GR. Improvement of reading frame maintenance is a common function for several tRNA modifications. Embo J 2001;20:4863–4873. [PubMed: 11532950]
22. Zhang CM, Perona JJ, Ryu K, Francklyn C, Hou YM. Distinct Kinetic Mechanisms of the Two Classes of Aminoacyl-tRNA Synthetases. J Mol Biol 2006;361:300–311. [PubMed: 16843487]
23. Holmes WM, Andraos-Selim C, Roberts I, Wahab SZ. Structural requirements for tRNA methylation. Action of Escherichia coli tRNA(guanosine-1)methyltransferase on tRNA(1Leu) structural variants. J Biol Chem 1992;267:13440–13445. [PubMed: 1618846]
24. Hou YM, Li Z, Gamper H. Isolation of a site-specifically modified RNA from an unmodified transcript. Nucleic Acids Res 2006;34:e21. [PubMed: 16473844]
25. Ibba M, Soll D. Aminoacyl-Trna Synthesis. Annu Rev Biochem 2000;69:617–650. [PubMed: 10966471]
26. Rould MA, Perona JJ, Soll D, Steitz TA. Structure of E. coli glutaminyl-tRNA synthetase complexed with tRNA(Gln) and ATP at 2.8 A resolution [see comments]. Science 1989;246:1135–1142. [PubMed: 2479982]
27. Belrhali H, Yaremchuk A, Tukalo M, Larsen K, Berthet-Colominas C, Leberman R, Beijer B, Sproat B, Als-Nielsen J, Grubel G, et al. Crystal structures at 2.5 angstrom resolution of seryl-tRNA synthetase complexed with two analogs of seryl adenylate. Science 1994;263:1432–1436. [PubMed: 8128224]
28. Guth E, Connolly SH, Bovee M, Francklyn CS. A substrate-assisted concerted mechanism for aminoacylation by a class II aminoacyl-tRNA synthetase. Biochemistry 2005;44:3785–3794. [PubMed: 15751955]
29. Guth EC, Francklyn CS. Kinetic discrimination of tRNA identity by the conserved motif 2 loop of a class II aminoacyl-tRNA synthetase. Mol Cell 2007;25:531–542. [PubMed: 17317626]
30. Lindstrom WM Jr, Flynn J, Reich NO. Reconciling structure and function in HhaI DNA cytosine-C-5 methyltransferase. J Biol Chem 2000;275:4912–4919. [PubMed: 10671528]
31. Vilkaitis G, Merkiene E, Serva S, Weinhold E, Klimasauskas S. The mechanism of DNA cytosine-5 methylation. Kinetic and mutational dissection of Hhai methyltransferase. J Biol Chem 2001;276:20924–20934. [PubMed: 11283006]
32. Bhattacharya SK, Dubey AK. Kinetic mechanism of cytosine DNA methyltransferase MspI. J Biol Chem 1999;274:14743–14749. [PubMed: 10329670]
33. Flynn J, Glickman JF, Reich NO. Murine DNA cytosine-C5 methyltransferase: pre-steady- and steady-state kinetic analysis with regulatory DNA sequences. Biochemistry 1996;35:7308–7315. [PubMed: 8652507]
34. Sauerwald A, Zhu W, Major TA, Roy H, Palioura S, Jahn D, Whitman WB, Yates JR 3rd, Ibba M, Soll D. RNA-dependent cysteine biosynthesis in archaea. Science 2005;307:1969–1972. [PubMed: 15790858]
35. Fukunaga R, Yokoyama S. Structural insights into the first step of RNA-dependent cysteine biosynthesis in archaea. Nat Struct Mol Biol 2007;14:272–279. [PubMed: 17351629]
36. Kamtekar S, Hohn MJ, Park HS, Schnitzbauer M, Sauerwald A, Soll D, Steitz TA. Toward understanding phosphoseryl-tRNACys formation: the crystal structure of Methanococcus maripaludis phosphoseryl-tRNA synthetase. Proc Natl Acad Sci U S A 2007;104:2620–2625. [PubMed: 17301225]
37. Wu JC, Santi DV. Kinetic and catalytic mechanism of HhaI methyltransferase. J Biol Chem 1987;262:4778–4786. [PubMed: 3558369]
38. Merkiene E, Klimasauskas S. Probing a rate-limiting step by mutational perturbation of AdoMet binding in the HhaI methyltransferase. Nucleic Acids Res 2005;33:307–315. [PubMed: 15653631]
39. Schubert HL, Blumenthal RM, Cheng X. Many paths to methyltransfer: a chronicle of convergence. Trends Biochem Sci 2003;28:329–335. [PubMed: 12826405]
40. Cheng X, Kumar S, Posfai J, Pflugrath JW, Roberts RJ. Crystal structure of the HhaI DNA methyltransferase complexed with S-adenosyl-L-methionine. Cell 1993;74:299–307. [PubMed: 8343957]
41. Klimasauskas S, Kumar S, Roberts RJ, Cheng X. HhaI methyltransferase flips its target base out of the DNA helix. Cell 1994;76:357–369. [PubMed: 8293469]

42. O'Gara M, Klimasauskas S, Roberts RJ, Cheng X. Enzymatic C5-cytosine methylation of DNA: mechanistic implications of new crystal structures for HhaL methyltransferase-DNA-AdoHcy complexes. J Mol Biol 1996;261:634–645. [PubMed: 8800212]
43. Fersht AR, Ashford JS, Bruton CJ, Jakes R, Koch GL, Hartley BS. Active site titration and aminoacyl adenylate binding stoichiometry of aminoacyl-tRNA synthetases. Biochemistry 1975;14:1–4. [PubMed: 1109585]
44. Ambrogelly A, Kamtekar S, Stathopoulos C, Kennedy D, Soll D. Asymmetric behavior of archaeal prolyl-tRNA synthetase. FEBS Lett 2005;579:6017–6022. [PubMed: 16226256]
45. Guth E, Farris M, Bovee M, Francklyn CS. Asymmetric amino acid activation by class II histidyl-tRNA synthetase from Escherichia coli. J Biol Chem 2009;284:20753–20762. [PubMed: 19487703]
46. Fersht AR, Mulvey RS, Koch GL. Ligand binding and enzymic catalysis coupled through subunits in tyrosyl-tRNA synthetase. Biochemistry 1975;14:13–18. [PubMed: 162826]
47. Braeken K, Moris M, Daniels R, Vanderleyden J, Michiels J. New horizons for (p)ppGpp in bacterial and plant physiology. Trends Microbiol 2006;14:45–54. [PubMed: 16343907]
48. Noma A, Kirino Y, Ikeuchi Y, Suzuki T. Biosynthesis of wybutosine, a hyper-modified nucleoside in eukaryotic phenylalanine tRNA. Embo J 2006;25:2142–2154. [PubMed: 16642040]
49. Bailly M, Blaise M, Lorber B, Becker HD, Kern D. The transamidosome: A dynamic ribonucleoprotein particle dedicated to prokaryotic tRNA-dependent asparagine biosynthesis. Mol Cell 2007;26:228–239. [PubMed: 17964262]
50. Dupasquier M, Kim S, Halkidis K, Gamper H, Hou YM. tRNA integrity is a prerequisite for rapid CCA addition: implication for quality control. J Mol Biol 2008;379:579–588. [PubMed: 18466919]
51. Schmitt E, Moulinier L, Fujiwara S, Imanaka T, Thierry JC, Moras D. Crystal structure of aspartyl-tRNA synthetase from Pyrococcus kodakaraensis KOD: archaeon specificity and catalytic mechanism of adenylate formation. EMBO J 1998;17:5227–5237. [PubMed: 9724658]

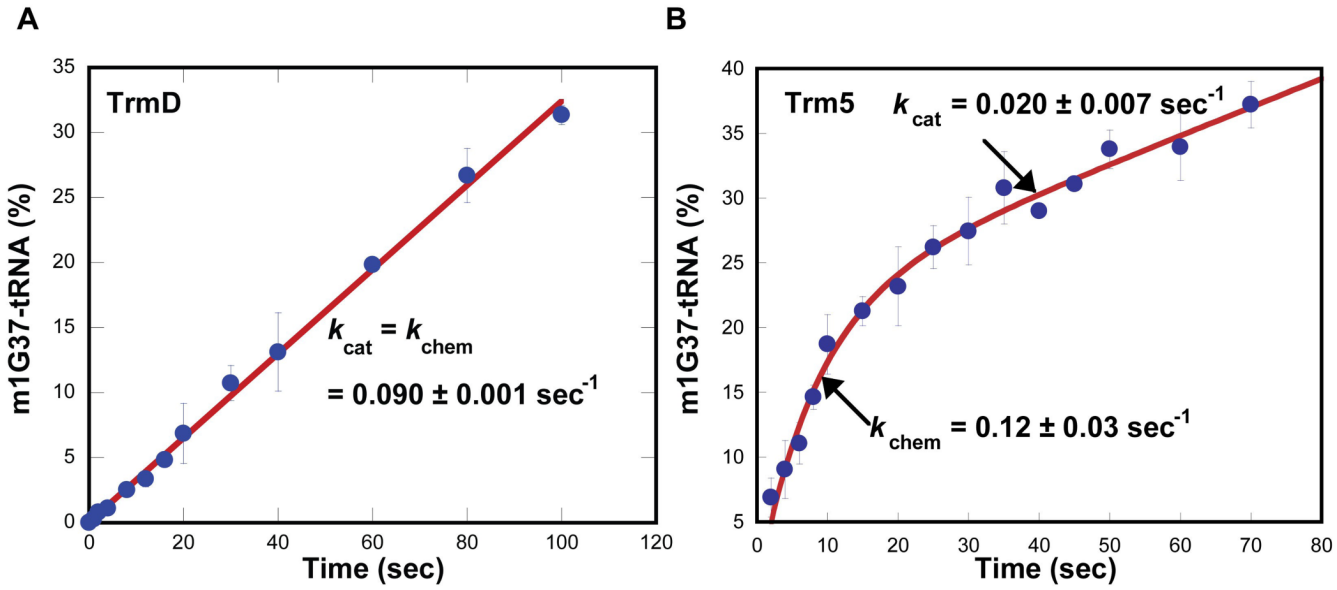

Figure 1.

Pre-steady-state analysis of m1G37-tRNA synthesis of TrmD and Trm5. (A) Time course of m1G37-tRNA synthesis was determined by mixing *E. coli* TrmD (1 μM) with *E. coli* $tRNA^{Leu}$ (10 μM) and AdoMet (30 μM) at 37°C. The time dependence of product formation, calculated as the amount of synthesis per active site of the enzyme (%), was fit to a linear equation to derive k_{cat}. (B) Time course of m1G37-tRNA synthesis was performed at 55°C as in (A) with *M. jannaschii* Trm5 (1 μM), *M. jannaschii* $tRNA^{cys}$ (10 μM), and AdoMet (25 μM). The data was fit to a burst equation by non-linear regression to derive k_{chem} and k_{cat}.

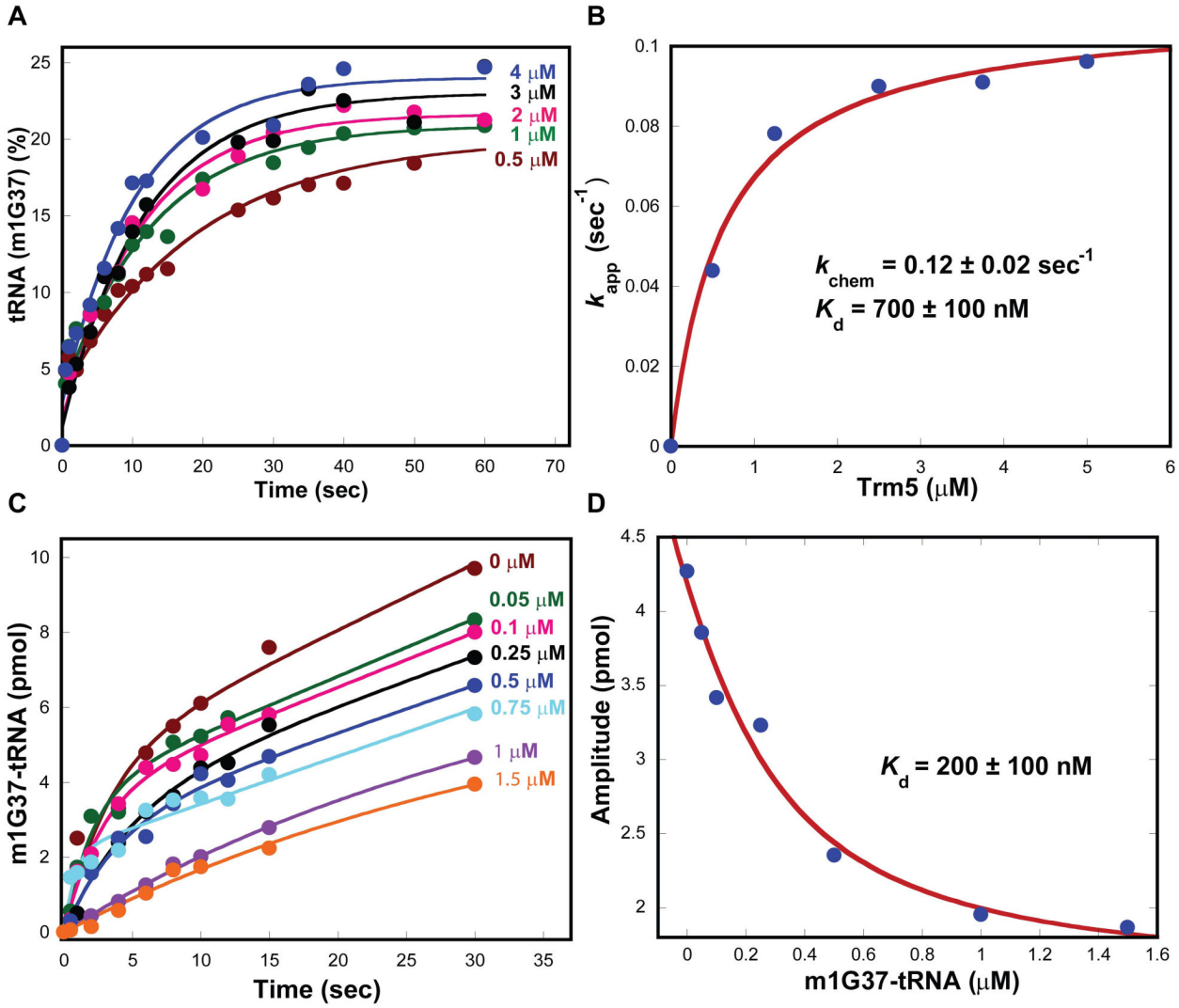

Figure 2.

Determination of tRNA parameters of Trm5. (A) Single turnover kinetics of the m1G37 synthesis reaction at 55°C performed at the indicated concentrations of *M. jannaschii* Trm5 with tRNA (0.25 mM) and AdoMet (25 μM). (B) Plot of the rate *vs*. concentration data fit to a hyperbolic equation to derive k_{chem} and K_d for tRNA. (C) Pre-steady-state kinetics of the m1G37 synthesis reaction by *M. jannaschii* Trm5 (1 μM)-m1G37-tRNA (0–1.5 μM) complexes with tRNA (10 μM) and AdoMet (50μM). (D) Plot of the rate *vs*. concentration data fit to a quadratic equation to deriveK_d for m1G37-tRNA.

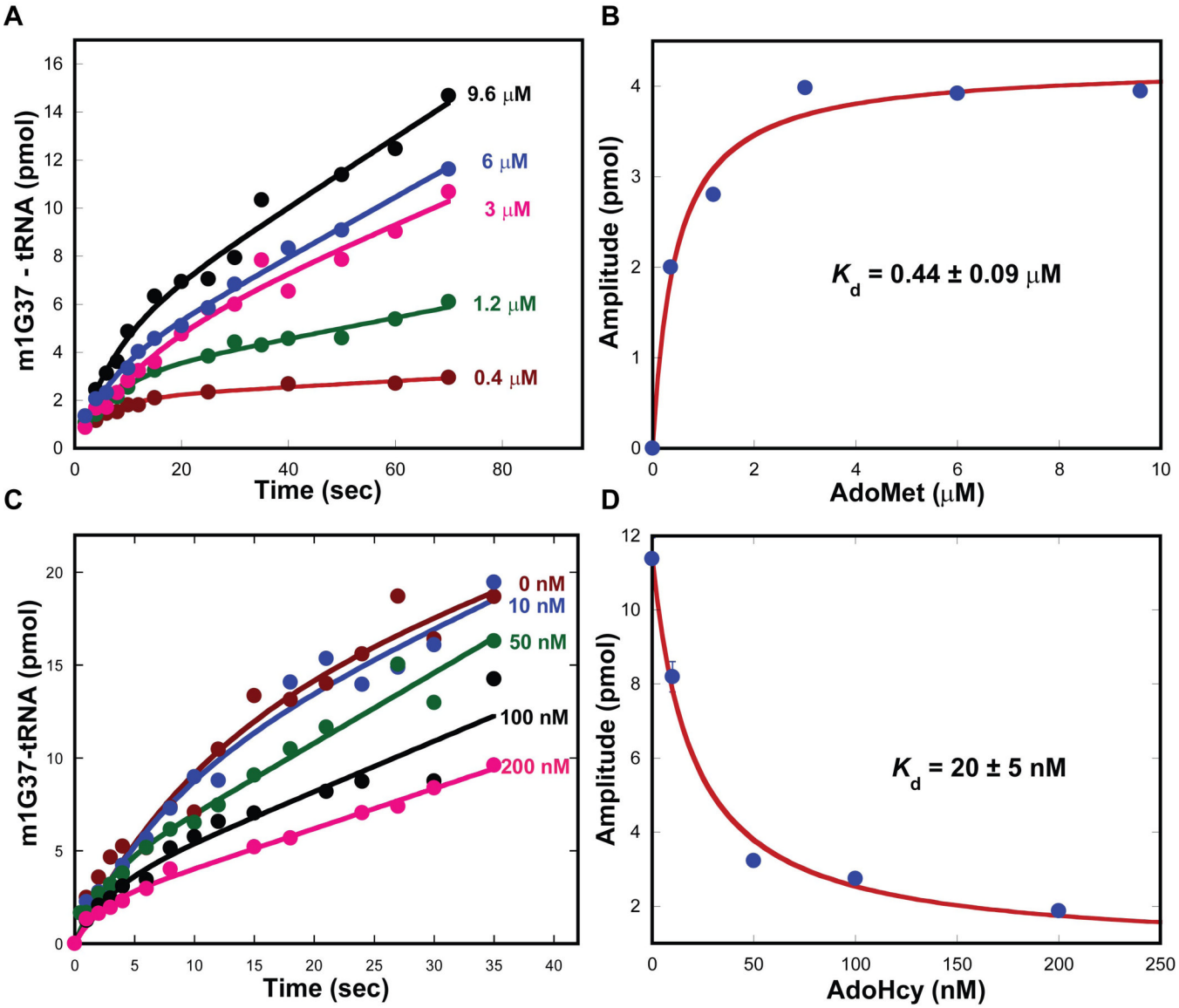

Figure 3.

Determination of AdoMet parameters of Trm5. (A) Pre-steady-state kinetics of the m1G37 synthesis reaction by rapidly mixing *M. jannaschii* Trm5 (5 μM)-AdoMet (0.4–9.6 μM) complexes with tRNA (15 μM). (B) Plot of the rate *vs*. concentration data of (A) fit to a hyperbolic equation to derive the K_d for tRNA. (C) Pre-steady-state kinetics of the m1G37 synthesis reaction by rapidly mixing *M. jannaschii* Trm5 (5 μM)-AdoHcy (0–0.2 μM) complexes with tRNA (15 μM) and AdoMet (25 μM). (D) Plot of the data of (C) fit to a hyperbolic equation to derive K_d for AdoHcy.

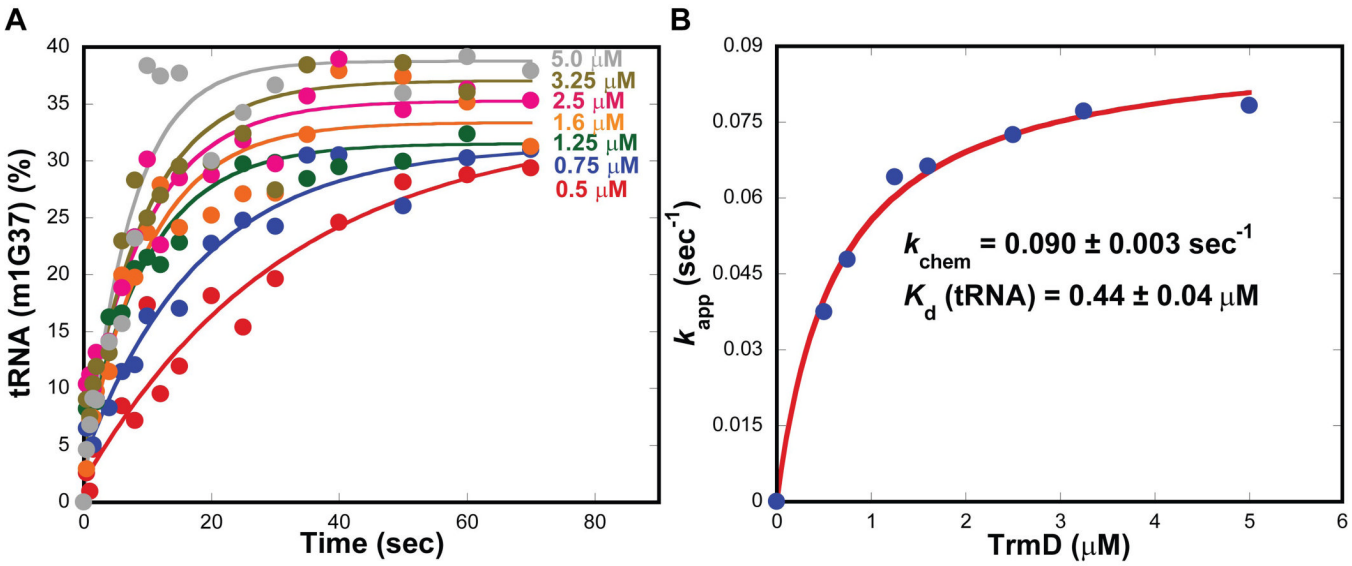

Figure 4.

Single turnover kinetics of TrmD. (A) Single turnover kinetics of the m1G37 synthesis reaction at 37°C performed at the indicated concentrations of *E. coli* TrmD with tRNA (0.25 μM) and AdoMet (30 μM). (B) Plot of the rate *vs*. concentration data fit to a hyperbolic equation to derive the k_{chem} of the reaction and the K_d for tRNA.

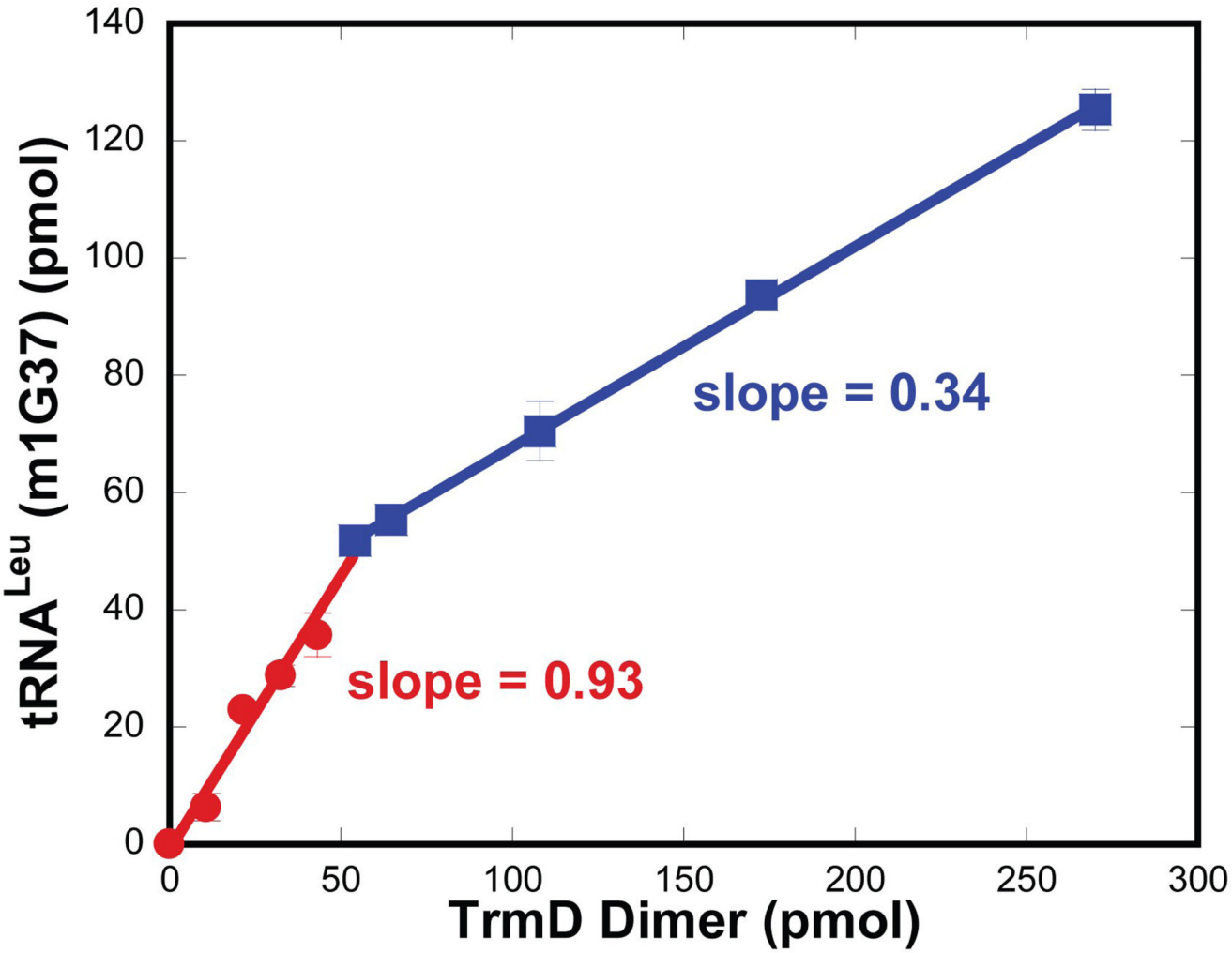

Figure 5.

Stoichiometry of methyl transfer of TrmD. The amount of m1G37-tRNA synthesis was measured at 37°C in single turnover conditions, where saturating tRNA (5 μM) and AdoMet (30 μM) were rapidly mixed with TrmD dimer (active concentration 0.36–9 μM). The reaction was acid quenched at 11 seconds. The amount of product formed was plotted against the active concentration of TrmD dimer, generating two linear fits with slopes of 0.93 and 0.33, respectively. The inflection point occurred at a ratio of 1 of tRNA:TrmD dimer.

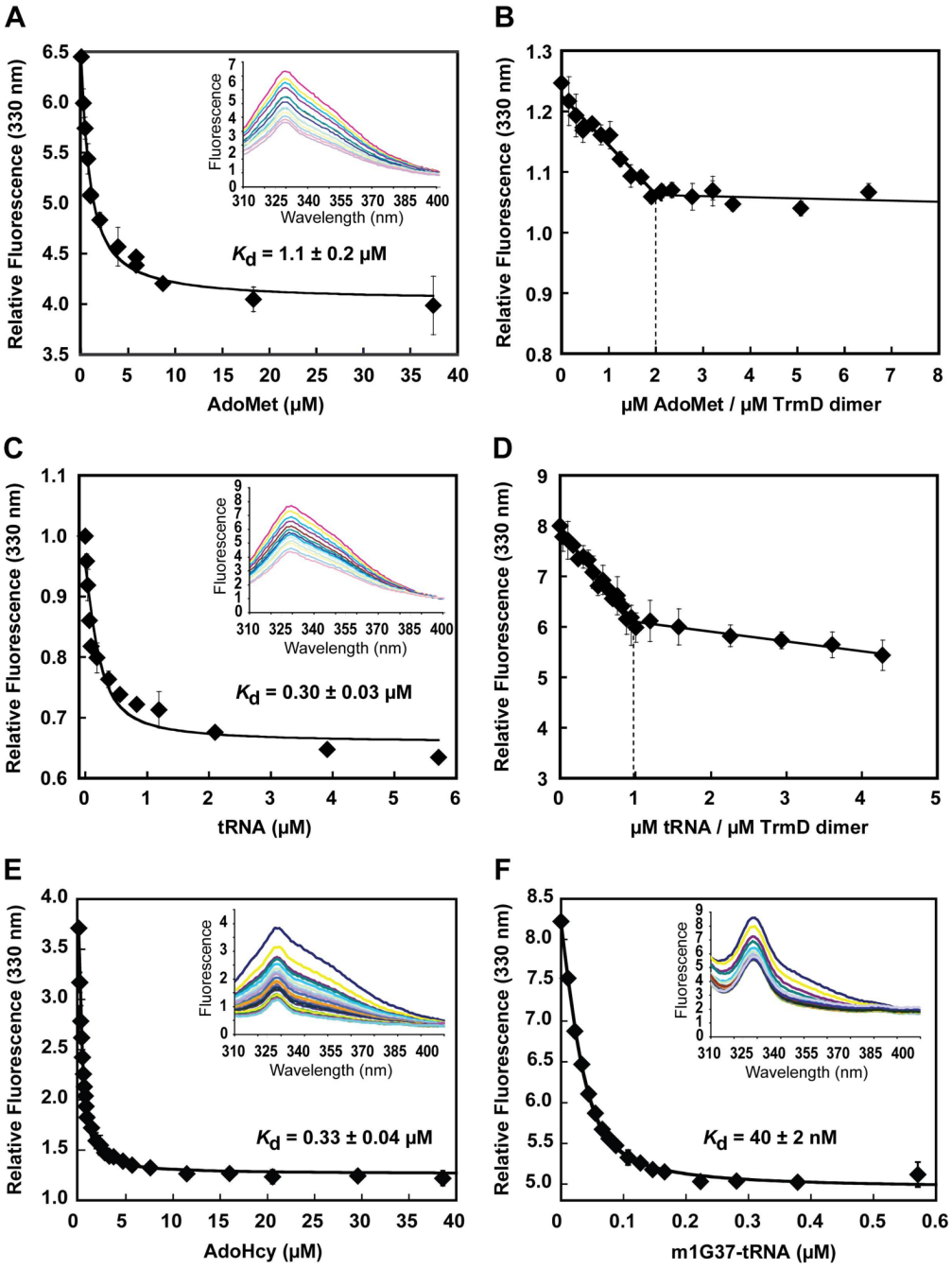

Figure 6.

Determination of substrate stoichiometry of TrmD. (A) Quenching of intrinsic tryptophan fluorescence of TrmD by AdoMet binding with emission scans shown in inset. A quadratic fit of quenching (at 330 nm) *vs*. AdoMet concentration revealed a K_d of 1.1 ± 0.2 μM. (B) Determination of the stoichiometry of AdoMet by tryptophan fluorescence quenching. (C) Quenching of intrinsic tryptophan fluorescence of TrmD by tRNA binding with emission scans shown in inset. A quadratic fit of quenching (at 330 nm) *vs*. tRNA concentration revealed a K_d of 0.3 ± 0.03 μM. (D) Determination of the stoichiometry of tRNA by tryptophan fluorescence quenching. (E) Quenching of intrinsic tryptophan fluorescence of TrmD by AdoHcy binding with emission scans shown in inset. A quadratic fit of quenching (at 330 nm)

vs. AdoHcy concentration revealed a K_d of 0.33 ± 0.04 μM. (F) Quenching of intrinsic tryptophan fluorescence of TrmD by binding of m1G37-tRNA with emission scans shown in inset. A quadratic fit of quenching (at 330 nm) *vs*. tRNA concentration revealed a K_d of 40 ± 2 nM. Error bars represent ± SD from two to three independent titrations.

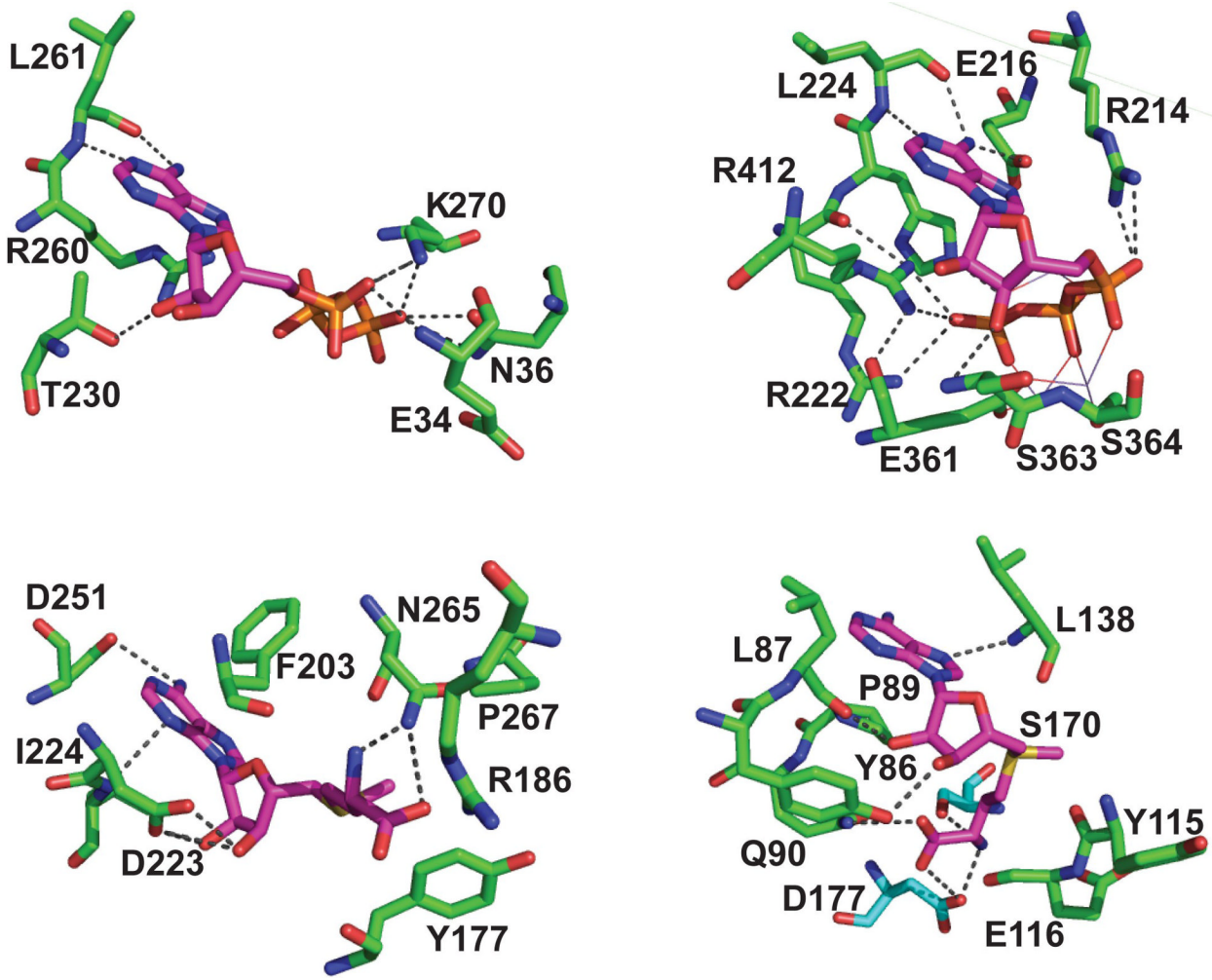

Figure 7.

Active-site structural similarities between AdoMet-dependent methyl transferases and ATP-dependent aminoacyl-tRNA synthetases. (A) Active site of *M. jannaschii* Trm5 in complex with AdoMet (PDB ID:2ZZN) [9]. (B) Active site of *Haemophilus influenzae* TrmD in complex with AdoMet (PDB ID:1UAK) [4]. (C) Active site of the class I *E. coli* GlnRS in complex with ATP complex (PDB ID:1GTR) [26]. (D) Active site of the class II *Pyrococcus kodakaraensis* AspRS in complex with a U-shaped ATP (PDB ID:1B8A) [51]. All structures show the conserved residues that stabilize the specific conformation of the cofactor, which exhibits an extended conformation in (A) and (C) and in a U-shaped conformation in (B) and (D).

Table 1

Parameters of the synthesis of m1G37-tRNA

	k_{chem} (sec^{-1})	k_{cat} (sec^{-1})	K_d (tRNA) (μM)	K_d (m1G37-tRNA) (μM)	K_d (AdoMet) (μM)	K_d (AdoHcy) (μM)
Trm5 (K)	0.12 ± 0.02	0.020 ± 0.007	0.7 ± 0.1	0.2 ± 0.1	0.44 ± 0.09	0.020 ± 0.005
TrmD (K)	0.090 ± 0.003	0.090 ± 0.001	0.44 ± 0.04			
TrmD (F)			0.30 ± 0.03	0.04 ± 0.002	1.1 ± 0.2	0.33 ± 004

E. coli TrmD and *M. jannaschii* Trm5 were analyzed for kinetic parameters at 37 °C and 55 °C, respectively, for the reaction of synthesis of m1G37 on *E. coli* $tRNA^{Leu}$ and *M. jannaschii* $tRNA^{Cys}$. The reported values represent the mean ± SD of at least two independent measurements. Note that values in the rows of Trm5 (K) and TrmD (K) were obtained from kinetic analysis, while those in the row of TrmD (F) were obtained by fluorescence titration of binding analysis.